shRNA targeting α-synuclein prevents neurodegeneration in a Parkinson's disease model

Alevtina D. Zharikov,[1,2,3] Jason R. Cannon,[1,2,3] Victor Tapias,[1,2] Qing Bai,[1,2] Max P. Horowitz,[1,2] Vipul Shah,[1,2] Amina El Ayadi,[1,2] Teresa G. Hastings,[1,2] J. Timothy Greenamyre,[1,2,3] and Edward A. Burton[1,2,3,4]

[1]Pittsburgh Institute for Neurodegenerative Diseases and [2]Department of Neurology, University of Pittsburgh School of Medicine, Pittsburgh, Pennsylvania, USA. [3]Geriatric Research Education and Clinical Center, VA Pittsburgh Healthcare System, Pittsburgh, Pennsylvania, USA. [4]Department of Microbiology and Molecular Genetics, University of Pittsburgh School of Medicine, Pittsburgh, Pennsylvania, USA.

Multiple convergent lines of evidence implicate both α-synuclein (encoded by *SCNA*) and mitochondrial dysfunction in the pathogenesis of sporadic Parkinson's disease (PD). Occupational exposure to the mitochondrial complex I inhibitor rotenone increases PD risk; rotenone-exposed rats show systemic mitochondrial defects but develop specific neuropathology, including α-synuclein aggregation and degeneration of substantia nigra dopaminergic neurons. Here, we inhibited expression of endogenous α-synuclein in the adult rat substantia nigra by adeno-associated virus–mediated delivery of a short hairpin RNA (shRNA) targeting the endogenous rat *Snca* transcript. Knockdown of α-synuclein by ~35% did not affect motor function or cause degeneration of nigral dopaminergic neurons in control rats. However, in rotenone-exposed rats, progressive motor deficits were substantially attenuated contralateral to α-synuclein knockdown. Correspondingly, rotenone-induced degeneration of nigral dopaminergic neurons, their dendrites, and their striatal terminals was decreased ipsilateral to α-synuclein knockdown. These data show that α-synuclein knockdown is neuroprotective in the rotenone model of PD and indicate that endogenous α-synuclein contributes to the specific vulnerability of dopaminergic neurons to systemic mitochondrial inhibition. Our findings are consistent with a model in which genetic variants influencing α-synuclein expression modulate cellular susceptibility to environmental exposures in PD patients. shRNA targeting the *SNCA* transcript should be further evaluated as a possible neuroprotective therapy in PD.

Introduction

Parkinson's disease (PD) is characterized pathologically by degeneration of discrete groups of neurons in the central, autonomic, and enteric nervous systems; the cardinal motor signs of PD (tremor, rigidity, and bradykinesia) are caused by loss of substantia nigra dopaminergic neurons, which are particularly vulnerable to pathogenesis (1). Some remaining neurons show intracellular inclusions — Lewy bodies and Lewy neurites — containing deposits of insoluble α-synuclein (2–4). Variants in the *SNCA* gene, encoding α-synuclein, modulate both PD risk (5–7) and α-synuclein expression levels (8), suggesting that α-synuclein may be involved in pathogenesis. This is supported by rare Mendelian PD phenocopies caused by *SNCA* gene duplications (9) and triplications (10) that increase α-synuclein expression levels (11) and by *SNCA* missense mutations that alter the amino acid sequence and biophysical properties of α-synuclein (12–14). However, common *SNCA* variants are insufficient to cause PD alone; other factors, including environmental exposures, contribute significantly to pathogenesis.

An important role for mitochondrial dysfunction in the pathogenesis of PD is suggested by the following observations: multiple tissues from PD patients show deficits in mitochondrial function, particularly complex I of the respiratory chain (15, 16); the substantia nigra in PD shows consumption of endogenous antioxidants and

severe oxidative damage (17); loss-of-function mutations in several genes encoding proteins with mitochondrial functions cause early-onset parkinsonism (18–20); there is a strong epidemiological association between risk of PD and occupational exposure to rotenone, a naturally occurring pesticide that is a potent inhibitor of complex I of the mitochondrial respiratory chain (21); and an unusual form of acute parkinsonism was caused in a small number of patients by MPTP (1-methyl-4-phenyl-1,2,3,6-tetrahydropyridine), which is metabolized in the CNS to yield a mitochondrial complex I inhibitor, MPP+ (1-methyl-4-phenylpyridinium) (22).

It is currently unclear how abnormalities of mitochondrial function and α-synuclein interact in the pathogenesis of PD. Overexpression of α-synuclein in cultured cells may alter mitochondrial function (23, 24), and oxidative stress resulting from mitochondrial impairment can influence α-synuclein expression and aggregation (25, 26). *Snca*−/− mice showed attenuated ROS production following inhibition of mitochondrial complex II with 3-nitropropionic acid (27). The dopaminergic neurons of some strains of *Snca*−/− mice were partially resistant to MPTP (28, 29). However, it is uncertain whether protection from MPTP is attributable to a pharmacokinetic mechanism unrelated to mitochondrial function. MPP+, the toxic metabolite of MPTP, is a substrate for the dopamine transporter (DAT), resulting in its selective uptake into dopaminergic terminals (30). Loss of α-synuclein has been reported to decrease cell surface expression of DAT in *Snca*−/− mice (31, 32) and cultured cells (33), which might attenuate MPTP toxicity by altering MPP+ uptake. However, studies showing that some strains of *Snca*−/− mice were protected against MPTP did not reveal any alteration in stri-
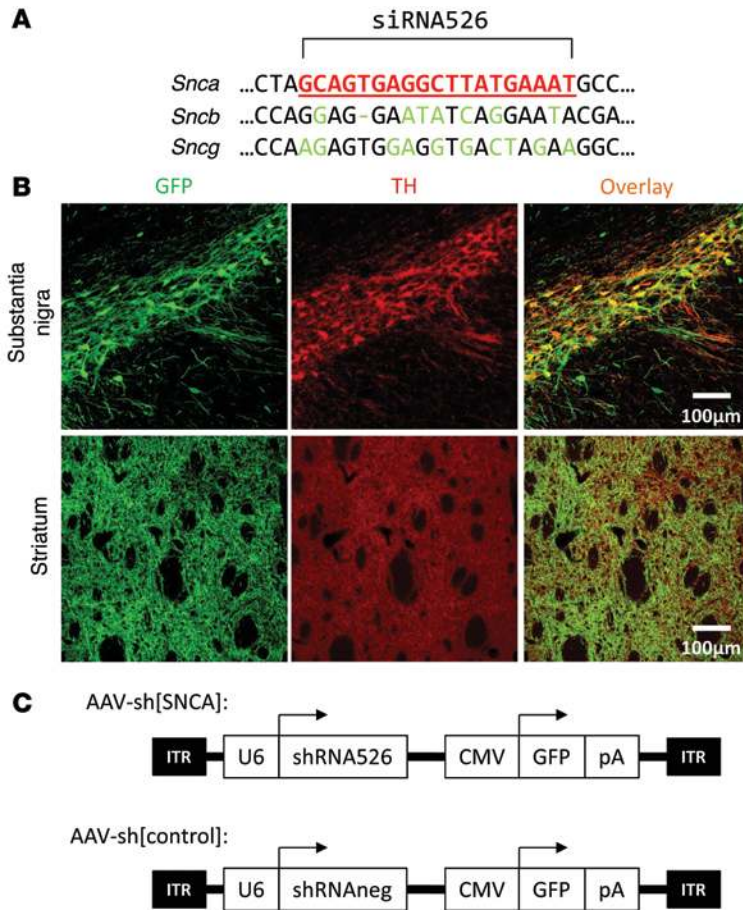
Figure 1. Generation of a viral vector to target endogenous α-synuclein in vivo. (**A**) siRNAs targeting *Snca* were identified and tested in vitro (Supplemental Figures 1–3). The most effective of these, siRNA526, is shown in red. Multiple base mismatches between siRNA526 and the corresponding sequences of *Sncb* and *Sncg* (encoding β- and γ-synucleins, respectively) are colored green. (**B**) A variety of viral vectors was evaluated for in vivo gene transfer to the rat substantia nigra (Supplemental Figure 4). An adeno-associated virus serotype 2 (AAV2) vector expressing a GFP reporter gene showed extensive transduction of TH⁺ nigral dopaminergic neurons (upper panels), with resulting GFP expression in their striatal terminals (lower panels). Scale bars: 100 μm. (**C**) An AAV2 vector, AAV-sh[SNCA], was constructed to express shRNA526 targeting *Snca* from the U6 promoter and a GFP reporter from a separate expression cassette. The control vector AAV-sh[control] was isogenic to AAV-sh[SNCA], except that it expressed a nontargeting shRNA instead of shRNA526.

nigrostriatal dopaminergic lesion caused by rotenone is associated with α-synuclein–immunoreactive inclusion body pathology reminiscent of Lewy bodies (36); and (ii) rotenone is highly lipophilic, and consequently its entry into cells is not dependent on expression of DAT that might be altered by decreasing α-synuclein levels.

In view of compelling evidence linking both α-synuclein and mitochondrial dysfunction to PD, we hypothesized that a critical pathogenic interaction between these factors occurs in vulnerable cell groups. We tested this hypothesis by asking whether reducing endogenous α-synuclein expression in the substantia nigra of adult rats prevented neurodegeneration in the rotenone model of PD. Our findings indicate that α-synuclein contributes to the selective vulnerability of nigral neurons to systemic mitochondrial complex I inhibition. This demonstrates a key mechanism for selective cell loss in PD and suggests that α-synuclein may be a valid target for further therapeutic development.

Results

Design and construction of a gene transfer vector targeting rat α-synuclein. We designed siRNAs to target regions of the rat *Snca* mRNA (encoding α-synuclein) that showed minimal homology to *Sncb* or *Sncg* (encoding β- and γ-synucleins, respectively). Sequences showing significant homology to other genes by BLAST search (http://blast.ncbi.nlm.nih.gov/Blast.cgi) were rejected. We tested three siRNAs that satisfied these design criteria in a subclone of Chinese hamster ovary (CHO) cells stably transfected to express rat α-synuclein (Supplemental Figures 1 and 2; supplemental material online with this article; doi:10:1172/JCI64502DS1). Expression of α-synuclein was robustly reduced in vitro by two of these sequences (siRNA270, 75% knockdown; siRNA526, 85% knockdown). siRNA526 was chosen for further studies because there are multiple mismatches between the *Snca*, *Sncb*, and *Sncg* genes at this location (Figure 1A). An shRNA corresponding to the sequence of siRNA526, expressed under transcriptional control of the U6 (RNA polymerase III) promoter, gave rise to progressive loss of α-synuclein expression in vitro (Supplemental Figure 3).

We compared a number of different vectors for transduction of the substantia nigra in vivo (40) (Supplemental Figure 4). Adeno-associated virus serotype 2 (AAV2) vectors, recently shown

atal DAT expression (28, 29), and the question of whether loss of α-synuclein protects from MPTP by impaired uptake of MPP⁺ or another mechanism remains unresolved.

Rats exposed chronically to rotenone show systemic reduction in the activity of complex I of the mitochondrial respiratory chain (34). The deficit is similar in magnitude to the systemic abnormalities in mitochondrial function reported in PD patients. Despite this systemic abnormality, rotenone-treated rats develop specific PD-like neuropathology, including progressive nigrostriatal degeneration and α-synuclein pathology (34). This model replicates many features of sporadic PD, including progressive parkinsonism responsive to dopaminergic medications; loss of dopaminergic neurons and their striatal terminals; depletion of endogenous antioxidants, oxidative damage to dopaminergic neurons, and iron deposition; microglial activation; and α-synuclein pathology in the enteric nervous system (34–37). In its original form, using intravenous administration via an osmotic minipump, the model was quite variable (34), and some researchers noted nonspecific systemic toxicity from rotenone (reviewed in ref. 38). However, recent refinements to this model — particularly the development of a reliable intraperitoneal delivery protocol using a triglyceride vehicle — have yielded more reproducible results, and rotenone has now been used in several species to model both motor and non-motor features of PD (reviewed in ref. 39). The rat rotenone model provides an appropriate setting in which to examine the role of endogenous α-synuclein in the pathogenesis of sporadic PD, because (i) the

Table 1. Animal cohorts, interventions and assays discussed in the text

Cohort	Experimental groups (no. rats)	Number of rats	Rotenone exposure	Analyses
1	Ipsilateral AAV-sh[SNCA] + contralateral sh[control]	3	No	α-Synuclein quantification in nigral dopaminergic neurons *Snca* RNA in situ hybridization in nigra TH quantification in striatum
2	Unilateral AAV-sh[SNCA] Unilateral AAV-sh[control]	5 5	No	Postural instability test Cylinder/rearing test α-Synuclein quantification in nigral dopaminergic neurons TH quantification in nigral dopaminergic neurons *Snca* RNA in situ hybridization in nigra TH quantification in striatum Stereological quantification of nigral dopaminergic neurons
3	Unilateral AAV-sh[SNCA] Unilateral AAV-sh[control]	4 5	No	Striatal neurochemistry
4	No vector; Unilateral AAV-sh[SNCA] Unilateral AAV-sh[control]	6 6 6	2.8 mg/kg daily to motor end point	Postural instability test Cylinder/rearing test TH quantification in striatum Stereological quantification of nigral dopaminergic neurons Dopaminergic neuron neurite quantification α-Synuclein quantification in nigral dopaminergic neurons *Snca* RNA in situ hybridization in nigra TH quantification in nigral dopaminergic neurons
5	Ipsilateral AAV-sh[SNCA] + contralateral sh[control]	5	2.8 mg/kg daily to motor end point	TH quantification in striatum Stereological quantification of nigral dopaminergic neurons Dopaminergic neuron neurite quantification *Snca* RNA in situ hybridization in nigra
6	No vector Unilateral AAV-sh[SNCA] Unilateral AAV-sh[control]	8 8 8	2.8 mg/kg daily for 6 days	Postural instability test TH quantification in striatum *Snca* RNA in situ hybridization in nigra

to be safe in PD gene therapy clinical trials (41, 42), showed robust transgene expression in rat dopaminergic neurons and their striatal terminals (Figure 1B). An AAV2 vector (AAV-sh[SNCA]; Figure 1C) was constructed to express both shRNA526 and GFP, facilitating identification of transduced neurons in subsequent experiments. The control vector, AAV-sh[control], encoded a nontargeting shRNA but was otherwise isogenic to AAV-sh[SNCA].

For initial in vivo evaluation of the vectors, AAV-sh[SNCA] was infused into the substantia nigra unilaterally and AAV-sh[control] was infused on the contralateral side (rat cohort 1; see Table 1 for summary of experimental cohorts, interventions, and assays). Three weeks after vector transduction, gene expression was evaluated by RNA in situ hybridization (Figure 2A). *Snca* mRNA was not detected in dopaminergic neurons of the substantia nigra on the side that received AAV-sh[SNCA], whereas AAV-sh[control] did not affect *Snca* expression (Figure 2A). Expression of *Sncb* and *Sncg* was unaffected by either vector (Figure 2A), showing that AAV-sh[SNCA] targeted *Snca* specifically.

The enrichment of α-synuclein at presynaptic terminals poses a technical challenge for quantification of the protein in substantia nigra dopaminergic neurons: the majority of α-synuclein immunoreactivity in the substantia nigra is localized to terminals of axonal projections from other brain regions. Furthermore, α-synuclein in the striatal terminals of nigral dopaminergic neurons lies in close proximity to other populations of terminals and neurons.

However, it was possible to measure the somatic component of α-synuclein immunoreactivity within tyrosine hydroxylase–expressing (TH-expressing) nigral neurons by confocal microscopy (Figure 3, A and B; Supplemental Figure 5). We quantified α-synuclein immunoreactivity in rats that received either AAV-sh[SNCA] or AAV-sh[control] unilaterally (cohort 2). Relative to nontransduced cells on the control side of the brain, α-synuclein expression in AAV-sh[SNCA]–transduced nigral dopaminergic neurons was reduced by ≈35% six weeks after surgery, whereas no change in α-synuclein expression was noted in neurons transduced with AAV-sh[control] (Figure 3, C and D). A similar reduction in α-synuclein expression was found in AAV-sh[SNCA]–transduced dopaminergic neurons in direct comparison with AAV-sh[control]–transduced neurons in animals that received bilateral vector transduction (cohort 1; Supplemental Figure 6).

Together these data show that AAV-sh[SNCA] caused a robust and specific reduction in *Snca* mRNA in substantia nigra dopaminergic neurons by 3 weeks after transduction and ≈35% loss of α-synuclein protein by 6 weeks after transduction.

Specific α-synuclein knockdown in vivo does not cause loss of nigral dopaminergic neurons or their striatal terminals. A unilateral transduction design, in which separate animals received either AAV-sh[SNCA] or AAV-sh[control], was employed to reveal the impact of each vector independently on animal health (cohort 2). This allowed us to evaluate for possible toxic effects resulting from α-synuclein
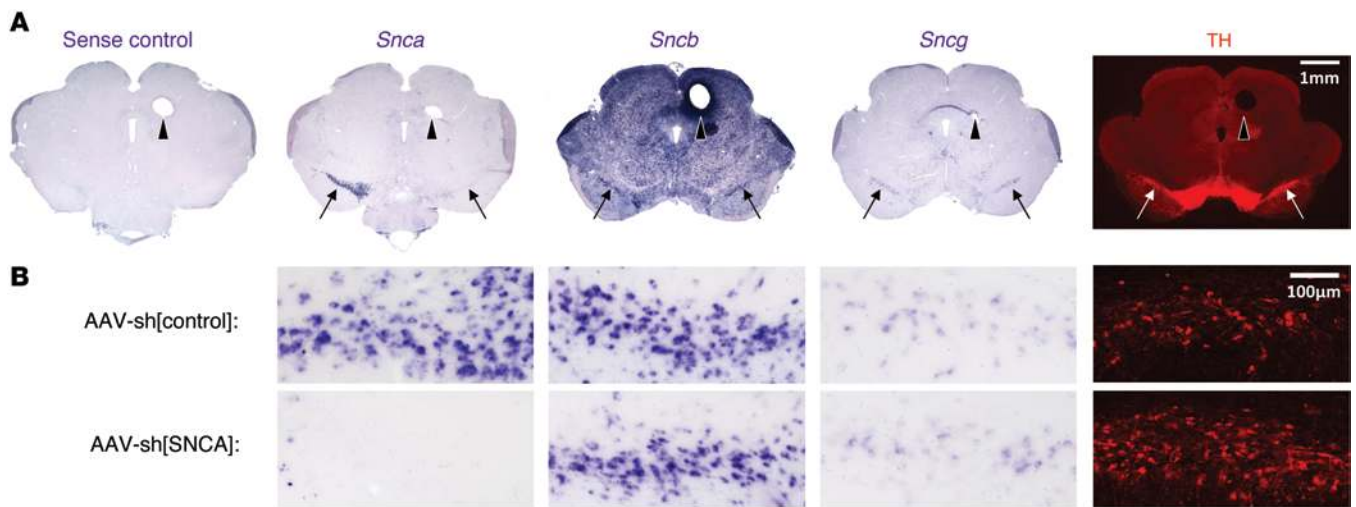
Figure 2. AAV-sh[SNCA] specifically targets *Snca* mRNA in the substantia nigra in vivo. The substantia nigra of three rats was transduced with AAV-sh[SNCA] on one side and AAV-sh[control] on the other (cohort 1). Twenty-one days later, contiguous midbrain sections were labeled by RNA in situ hybridization using antisense cRNA probes to *Snca*, *Sncb*, and *Sncg*; by a sense control probe; or by immunofluorescence for TH to label dopaminergic neurons. (**A**) Low-power micrographs of the midbrain. Arrows indicate the position of the substantia nigra, and arrowheads indicate punch marks labeling the side that received AAV-sh[SNCA]. Scale bar (for all panels): 1 mm. (**B**) The substantia nigra on each side of the corresponding section is shown at higher magnification. Specific loss of the *Snca* transcript is seen after transduction with AAV-sh[SNCA] but not AAV-sh[control]. Scale bar (for all panels): 100 μm.

knockdown. Immediate postoperative weight loss was identical in the two groups, and there were no significant differences in weight gain during the subsequent recovery period (Figure 4A). We evaluated both sets of animals for asymmetry in motor function that would indicate physiologically significant disturbances of nigral function provoked by vector transduction. We employed two complementary tests that are sensitive to dopaminergic function and useful for detecting unilateral deficits (36, 43, 44). The postural instability test evaluates evoked forepaw movements in a postural control paradigm, whereas the cylinder test evaluates spontaneous forepaw movements during exploration of a behavioral arena (43, 44). Neither AAV-sh[SNCA]– nor AAV-sh[control]–transduced animals showed any significant differences between left and right forepaw function in these tests at any time point up to 6 weeks after surgery (Figure 4, B–D).

We next analyzed the nigrostriatal system histologically. Unbiased stereology did not show loss of dopaminergic neurons in the AAV-sh[SNCA]–transduced substantia nigra relative to the control side that was not exposed to vector (Figure 5A). Confocal microscopy showed no significant difference in TH expression between nigral neurons on the nontransduced control side of the brain and neurons transduced with either AAV-sh[SNCA] or AAV-sh[control] (Figure 5, B and C). Quantitative near-infrared immunofluorescence (Supplemental Figure 7) showed no significant difference in striatal TH expression ipsilateral to nigral AAV-sh[SNCA] or AAV-sh[control] transduction compared with the nontransduced control side (Figure 5, D, E, and F).

Finally, we analyzed neurochemical end points following α-synuclein knockdown, in view of emerging evidence that α-synuclein may be involved in regulating dopamine storage and release at striatal terminals (31, 45). The substantia nigra was transduced unilaterally with either AAV-sh[SNCA] or AAV-sh[control] (cohort 3); dopamine and its metabolites were measured in freshly dis-

sected striatal tissue at 42 days after transduction. The striatum ipsilateral to nigral AAV-sh[SNCA] transduction showed ≈20% reduction in dopamine content compared with the nontransduced side, whereas no difference was apparent between the two sides in AAV-sh[control] animals (Figure 5F). Dopamine turnover, estimated by the ratio of the dopamine metabolites 3,4-dihydroxyphenylacetic acid (DOPAC) and homovanillic acid (HVA) to dopamine, was unchanged following α-synuclein knockdown (Figure 5G).

Together, these data provide no evidence that either vector transduction or knockdown of endogenous α-synuclein caused degeneration of substantia nigra dopaminergic neurons or their striatal terminals. However, α-synuclein knockdown caused a modest reduction in striatal dopamine content that was not attributable to reduced TH expression, and which did not result in any detectable deficit in motor function.

Loss of α-synuclein prevents progressive motor deficits in the rotenone model of PD. We next evaluated the role of α-synuclein in the pathogenesis of the rotenone model of PD. Experiments were conducted using both unilateral and bilateral transduction designs. In unilateral transduction experiments, rats received either AAV-sh[SNCA] or AAV-sh[control] in the substantia nigra on one side (cohort 4). This enabled us to evaluate the effects of α-synuclein knockdown and control vector on survival to end point and motor function in separate animals, in comparison with a third group of animals that did not receive vector. In bilateral transduction experiments, rats received AAV-sh[SNCA] in the substantia nigra on one side and AAV-sh[control] in the other (cohort 5). This enabled direct comparison between the knockdown and control vectors in histological end points. Since the nigrostriatal dopaminergic lesion and associated motor deficits resulting from chronic systemic rotenone exposure are characteristically bilateral and symmetric (36), the two sides of each animal were compared, both in motor assays and by assessment
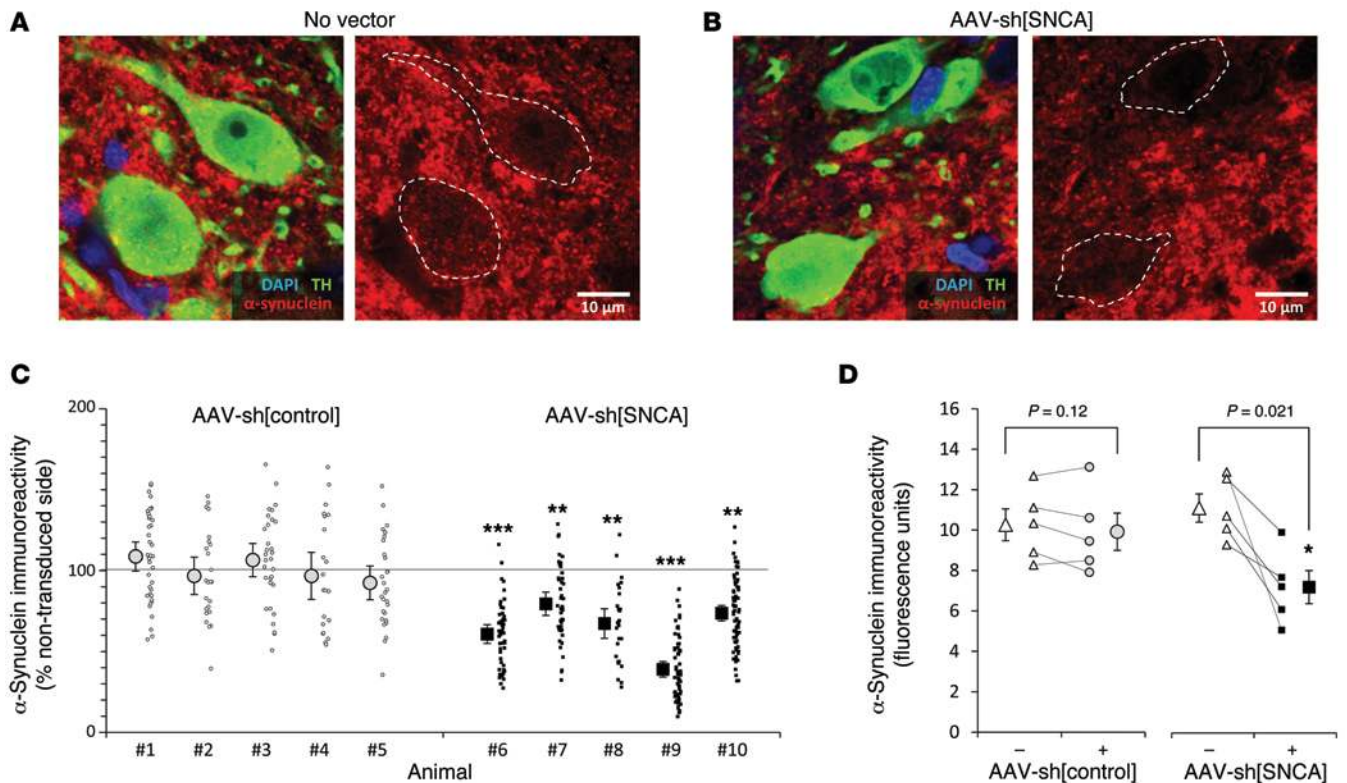
Figure 3. AAV-sh[SNCA] reduces α-synuclein expression in substantia nigra dopaminergic neurons. Two groups of 5 rats received either AAV-sh[SNCA] or AAV-sh[control] unilaterally in the substantia nigra (cohort 2). Forty-two days later, midbrain sections were immunolabeled for TH (green), α-synuclein (red), and DAPI (blue). Measurements of α-synuclein immunoreactivity were taken from nontransduced (white triangles), AAV-sh[control]–transduced (gray circles), or AAV-sh[SNCA]–transduced (black squares) substantia nigra dopaminergic neurons. (**A** and **B**) High-magnification confocal images of the substantia nigra from (**A**) no-vector and (**B**) AAV-sh[SNCA]–transduced sides of a single section. The positions of dopaminergic neuronal outlines revealed by TH labeling are shown as white dotted lines in the α-synuclein channel. Scale bars: 10 μm. (**C**) Cytoplasmic α-synuclein immunoreactivity was quantified in 60–100 nigral dopaminergic neurons on each side of each section by confocal imaging. The small markers show α-synuclein immunofluorescence signal for each cell on the vector-transduced side expressed as percentage of the mean value for dopaminergic neurons on the nontransduced side of the same section. The large markers show mean ± SEM for each animal. (**D**) Mean dopaminergic neuron α-synuclein immunofluorescence is shown for each side of the brain in each animal (+, vector side; –, nontransduced side; lines join the means for the two sides of each brain). The left graph shows measurements from animals that were transduced with AAV-sh[control] and the right AAV-sh[SNCA]. Large markers show mean ± SEM for all five animals in each group.*P < 0.05, **P < 0.01, ***P < 0.001, 2-tailed paired t test, vector transduced side versus control side.

of histological end points, to reveal the contribution of α-synuclein to pathogenesis. Analysis of samples from cohort 4 by quantitative confocal microscopy verified that AAV-sh[SNCA]–induced α-synuclein knockdown persisted following rotenone exposure (Supplemental Figure 8).

There was no difference in weight loss among no-vector control, AAV-sh[control]–, and AAV-sh[SNCA]–transduced rats during rotenone exposure (Figure 6A). There was also no difference in the time that rats from each experimental group were determined to have reached the approved study end point of >20% weight loss or severe generalized hypokinesia (Figure 6B). However, rats that received AAV-sh[SNCA] unilaterally in the right substantia nigra showed significant rescue of motor abnormalities in the contralateral left forelimb (Figure 6, C and D), which was not observed in the AAV-sh[control] or no-vector groups.

In the postural instability test, the displacement necessary to trigger a corrective forelimb movement is augmented when nigral dopaminergic function is impaired on the contralateral side. In rats that received either no vector or AAV-sh[control], the distance

to provoke a corrective movement increased progressively and symmetrically during rotenone exposure, from a mean baseline value of 3.1 cm to 5.2 cm by 8 days of rotenone exposure (this was the latest time point at which assays of motor function were carried out). In contrast, the left forelimbs of rats that received AAV-sh[SNCA] in the contralateral right substantia nigra showed only a small increase in the displacement necessary to provoke a corrective movement, from 3.1 cm at baseline to 3.6 cm by day 8 of rotenone exposure. The right forelimbs of the same animals showed an increase from 3.13 cm to 5.5 cm, similar to that observed in no-vector and AAV-sh[control] animals. The differences between AAV-sh[SNCA] animals and other experimental groups, and between the left and right forelimbs of AAV-sh[SNCA] animals, were statistically significant by day 4 of rotenone exposure. These differences became larger as rotenone-induced motor abnormalities progressed, and by day 6 were highly statistically significant (left forepaw of AAV-sh[SNCA] versus other groups, P = 0.00000016, 1-way ANOVA; right versus left forepaw of AAV-sh[SNCA] animals, P = 0.0000052, 2-tailed paired t test).
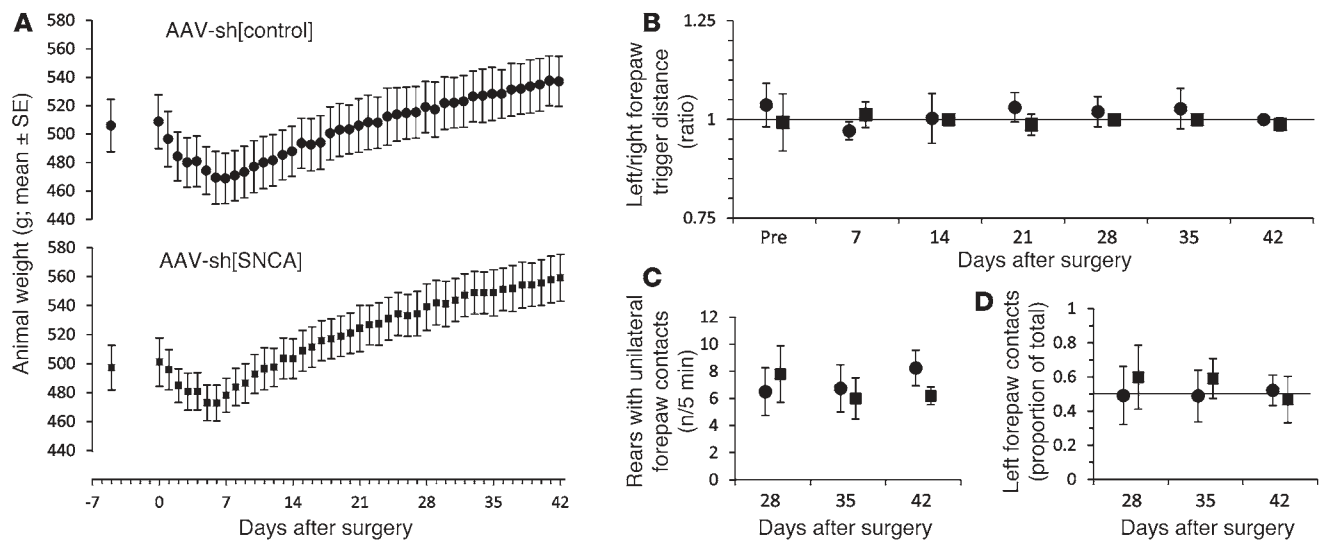
Figure 4. Absence of motor deficit following nigral α-synuclein knockdown. Animals from cohort 2 (unilateral AAV-sh[SNCA] or AAV-sh[control] into the substantia nigra) were analyzed for phenotypes attributable to α-synuclein knockdown. (**A**) The rats' weights were measured 7 days prior to stereotactic vector inoculation and then daily for 42 days thereafter. Data points show mean ± SEM. (**B**) A postural instability test was used to evaluate forelimb motor function. For each forelimb, the displacement of the rat necessary to provoke a compensatory forelimb movement was measured (see Methods). The ratio of this distance between the left and right forelimbs was determined at each time point shown. Data points show mean ± SEM for the AAV-sh[control] (gray circles) and AAV-sh[SNCA] (black squares) groups; the line shows ratio = 1 that would indicate perfectly symmetric motor function. Pre, before surgery. (**C** and **D**) Spontaneous exploratory behavior in a transparent cylinder was evaluated as a second test for forelimb motor function. (**C**) Rearing movements resulting in a unilateral forelimb contact with the cylinder wall were counted in each 5-minute time period. (**D**) The number of wall contacts made by the left forepaw was calculated as a percentage of the total unilateral forepaw contacts. Data points show mean ± SEM for the AAV-sh[control] (gray circles) and AAV-sh[SNCA] (black squares) groups. The line in **D** shows a value of 50% that would indicate perfectly symmetric motor function.

Spontaneous cylinder exploration was severely reduced from the onset of rotenone treatment as a result of systemic rotenone toxicity. Consequently, counting unilateral forepaw wall contacts during rearing behavior performed relatively poorly as a quantitative assay for motor asymmetry in this model. However, after 8 days of rotenone treatment, the remaining AAV-sh[SNCA] rats all showed some spontaneous exploratory behavior and rearing movements, whereas only one of the remaining AAV-sh[control] controls and none of the no-vector controls produced any spontaneous movements ($\chi^2 = 10.31$, $P < 0.05$). At this time point, AAV-sh[SNCA]–transduced rats showed significantly more rearing movements with unilateral left forelimb wall contacts than controls ($P = 0.0063$, 1-way ANOVA), whereas there was no significant difference in the number of rears with right forelimb wall contacts among the three groups.

Together, these data show that nigral α-synuclein knockdown prevented progressive loss of evoked contralateral forelimb movement, and partially rescued contralateral spontaneous forelimb movements, during chronic rotenone exposure.

α-Synuclein knockdown is neuroprotective in the rotenone model of PD. Neuropathological examination of samples from cohorts 4 and 5 showed that the preservation of neurological function contralateral to α-synuclein knockdown seen in cohort 4 was associated with neuroprotection on the side of the brain that received AAV-sh[SNCA] (Figures 7–9).

Loss of dopaminergic presynaptic terminals in the dorsolateral striatum was clearly visible in hemispheres that received AAV-sh[control] or no vector, similar to lesions previously reported in this model (36). In contrast, the striatum ipsilateral to

AAV-sh[SNCA] transduction did not show overt loss of striatal dopaminergic terminals (Figure 7, A and B). As an objective measure of striatal dopaminergic terminal integrity, quantitative near-infrared immunofluorescence was employed to measure dorsolateral striatal TH immunoreactivity in multiple tissue sections encompassing the rostrocaudal extent of the striatum (Supplemental Figure 7). Significant preservation of striatal dopaminergic terminals was found on the AAV-sh[SNCA]–transduced side compared with either the no-vector side (cohort 4; $P = 0.0097$, 2-tailed paired t test; Figure 7F) or the AAV-sh[control] side (cohort 5; $P = 0.0063$, 2-tailed paired t test; Figure 7D). In contrast, there was no significant difference between the AAV-sh[control] side and the no-vector side (cohort 4; $P = 0.629$, 2-tailed paired t test; Figure 7E). Furthermore, relative to the control left side, striatal TH immunoreactivity on the right side was significantly greater in animals that received unilateral AAV-sh[SNCA] than separate control animals that received AAV-sh[control] or no vector (Supplemental Figure 9A; cohort 4; $P = 0.016$, 1-way ANOVA). α-Synuclein knockdown thus protected striatal dopaminergic terminals from rotenone; overall, 25%–40% more TH signal was detected in the striatum ipsilateral to AAV-sh[SNCA] transduction than in control striatum at the experimental end point.

Severe rotenone-induced degeneration of substantia nigra dopaminergic neurons was observed in nontransduced and AAV-sh[control] samples. This neuronal loss was attenuated on the AAV-sh[SNCA] side in both cohorts 4 and 5 (Figure 8 and Supplemental Figure 9B). Unbiased stereological quantification confirmed that there were significantly more dopaminergic neurons remaining on the AAV-sh[SNCA] side compared with either the AAV-sh[control] side (cohort 5; $P = 0.007$, 2-tailed paired t test; Figure 8B) or no-vector
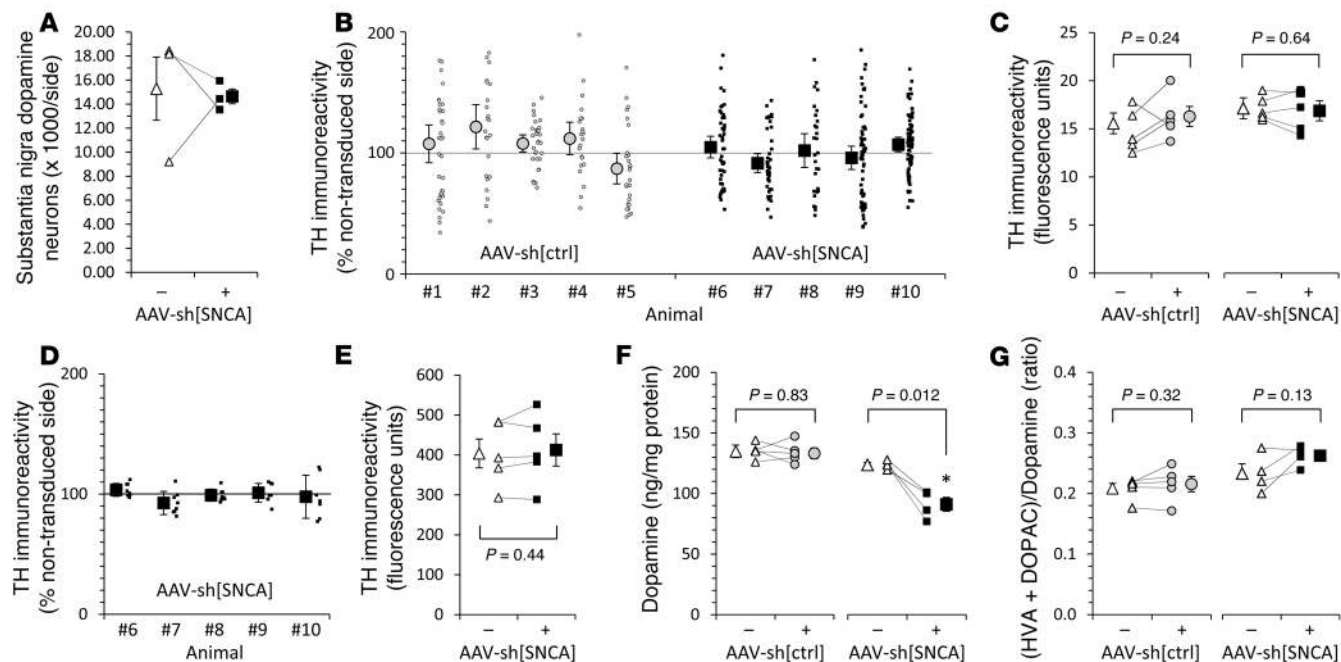
Figure 5. Preserved nigrostriatal morphology and TH expression, but reduced striatal dopamine content, following α-synuclein knockdown. Animals from cohorts 2 (**A**–**E**) and 3 (**F** and **G**) were analyzed for changes in the nigrostriatal system following unilateral α-synuclein knockdown. Measurements from the nontransduced (white triangles), AAV-sh[control]–transduced (gray circles), and AAV-sh[SNCA]–transduced (black squares) sides of each brain are shown. In **A**, **C**, and **E**–**G**, small markers show data points from each individual animal (the two sides of each brain are connected by a line); large markers show the group mean ± SEM. (**A**) Unbiased stereology was employed to quantify the number of nigral dopaminergic neurons on each side of the brain. (**B** and **C**) TH expression was measured in nigral dopaminergic neurons by confocal microscopy. In **B**, measurements for individual neurons are shown normalized to nontransduced cells in the same sections (small markers). Large markers show mean ± SEM for each animal. (**D** and **E**) Striatal TH expression was measured using quantitative near-infrared immunofluorescence. In **D**, measurements in individual sections are shown normalized to the nontransduced side of the same section (small markers). Large markers show mean ± SEM for each animal. (**F** and **G**) HPLC was employed to quantify dopamine levels (**F**) and the ratio of dopamine metabolites to dopamine (**G**) as an index of dopamine turnover. Data were analyzed using 2-tailed paired t tests comparing the vector-transduced and control sides of each brain; *$P < 0.05$.

side (cohort 4; $P = 0.01$, 2-tailed paired t test; Figure 8D). In contrast, there was no significant difference between the AAV-sh[control] and no-vector sides (cohort 4; $P = 0.6$, 2-tailed paired t test; Figure 8C). Furthermore, relative to the control nontransduced side, more nigral dopaminergic neurons survived in animals that received unilateral AAV-sh[SNCA] vector infusion than AAV-sh[control] (Supplemental Figure 9B; cohort 4; $P = 0.0077$, 2-tailed unpaired t test). There was no difference in TH immunoreactivity among surviving AAV-sh[SNCA]–transduced, AAV-sh[control]–transduced, and nontransduced nigral dopaminergic neurons (Supplemental Figure 10), suggesting that rotenone did not cause global TH downregulation that was rescued by AAV-sh[SNCA]. In addition, it has been shown previously that rotenone causes loss of nigral Nissl-stained neurons that parallels loss of nigral TH immunoreactive cells in this model (46). Consequently, the observed decrease in the number of TH-expressing cells following rotenone exposure represents neuronal loss, rather than TH downregulation. α-Synuclein knockdown thus protected nigral dopaminergic neurons from degeneration following exposure to rotenone; overall, 25%–30% more dopaminergic neurons remained in the AAV-sh[SNCA]–transduced side at the experimental end point compared with controls.

The dendritic processes of dopaminergic neurons remaining in the nontransduced and AAV-sh[control]–transduced substantia nigra following rotenone exposure showed evidence of severe dam-age. This was mitigated in AAV-sh[SNCA]–transduced substantia nigra. We measured the total length of neuritic processes per surviving dopaminergic neuron, using an automated algorithm, as an objective measure of dendritic integrity. Significant preservation of neurites was found in the AAV-sh[SNCA]–transduced side compared with either the no-vector side (cohort 4; $P = 0.0013$, 2-tailed paired t test; Figure 9D) or the AAV-sh[control] side (cohort 5; $P = 0.0068$, 2-tailed paired t test; Figure 9B). In contrast, there was no significant difference between the AAV-sh[control] side and the no-vector side (cohort 4; $P = 0.74$, 2-tailed paired t test; Figure 9C). Furthermore, relative to the control left side, the total length of processes per nigral dopaminergic neuron was greater in animals that received unilateral AAV-sh[SNCA] than separate control animals that received AAV-sh[control] (Supplemental Figure 9C; cohort 4; $P = 0.0078$, 2-tailed unpaired t test). α-Synuclein knockdown thus protected the dendrites of nigral dopaminergic terminals from rotenone; dopaminergic neurons in the AAV-sh[SNCA]–transduced substantia nigra showed overall 60% more total neurite length than controls. Similar differences between experimental groups were also found in neurite segments and branches (Supplemental Figure 11).

Together, these data show that α-synuclein knockdown protected substantia nigra dopaminergic neurons, their dendrites, and their striatal terminals from degeneration in the rotenone model of PD.
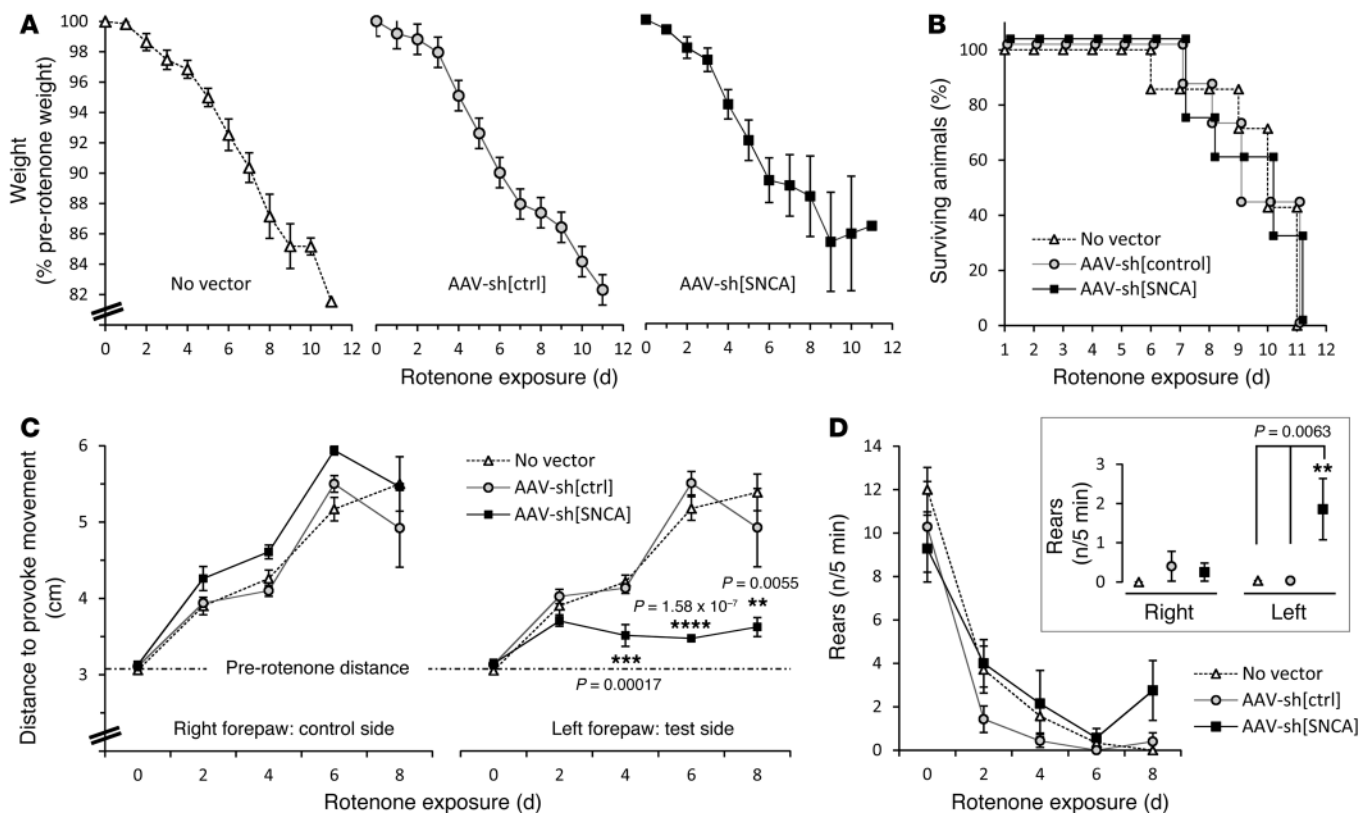
Figure 6. α-Synuclein knockdown protects motor function in the rotenone model of Parkinson's disease. Animals in cohort 4 received either AAV-sh[SNCA] (black squares) or AAV-sh[control] (gray circles) unilaterally in the substantia nigra, or no vector (white triangles). Starting at 21 days after transduction, rats were administered rotenone 2.8 mg/kg/d via intraperitoneal injection. (**A**) Weights were measured daily during rotenone administration. Data points show mean ± SEM expressed as percentage of initial starting weight for each animal. There were no significant differences in weight loss between the three groups. (**B**) Survival curve for time to predefined end points in the three experimental groups. (**C**) The postural instability test was used to evaluate forelimb motor function during rotenone administration. Mean ± SEM distance to trigger a compensatory forelimb movement is shown for the right forepaw (controlled by nontransduced side of brain; left graph) and left forepaw (controlled by vector-transduced side of brain; right graph). (**D**) Spontaneous exploratory behavior in a transparent cylinder was evaluated as a second test of forelimb motor function during rotenone administration. Mean ± standard error number of rearing movements is shown for each group. The inset panel shows rearing movements with unilateral wall contacts made by the right or left forelimbs after 8 days of rotenone exposure. **$P < 0.01$, ***$P < 0.005$, ****$P < 0.000001$, AAV-sh[SNCA] animals versus other groups, 1-way ANOVA with Tukey's post hoc test.

AAV-sh[SNCA] rescues function deficits that precede degeneration of striatal dopaminergic terminals. In order to better understand the events underlying neuroprotection, we examined the effects of α-synuclein knockdown on the integrity of dopaminergic terminals early in the clinical progression of the rotenone lesion (Figure 10). Eight animals in each group received either AAV-sh[SNCA] or AAV-sh[control] unilaterally in the substantia nigra (cohort 6) and were exposed to rotenone, as in cohort 4. However, brains were analyzed histologically after only 6 days of rotenone exposure, before any of the animals reached study end point. At this time point, there was prominent impairment of evoked forelimb motor function in the postural instability test in no-vector animals and contralateral to AAV-sh[control]–transduced substantia nigra, but motor function was preserved contralateral to the substantia nigra that received AAV-sh[SNCA] (AAV-sh[SNCA] versus other groups, $P = 6.4 \times 10^{-8}$, 1-way ANOVA; Figure 10A). No overt loss of TH labeling in the dorsolateral striatum was seen in any of the brains analyzed. Quantitative near-infrared immunofluorescence did not show any significant difference in striatal TH signal between the

control and AAV-sh[SNCA] sides (Figure 10, B and C), suggesting that the motor deficits found at this time point reflect loss of function rather than degeneration of striatal dopaminergic terminals. Consequently, we conclude that α-synuclein knockdown protects dopaminergic terminals from rotenone-induced functional impairment as an early event that precedes morphological abnormalities such as degeneration of nigral neurons and their terminals.

Discussion

We have demonstrated that knockdown of endogenous α-synuclein in the adult brain ameliorates pathology in an animal model of sporadic PD. Knockdown of the protein by ≈35% in the cell bodies of nigral dopaminergic neurons mitigated nigral α-synuclein accumulation, and protected motor function, striatal dopaminergic terminals, nigral dopaminergic neurons and their dendrites in the rotenone model of PD. These findings represent a significant advance in determining how genetic and environmental factors interact in PD pathogenesis, add to the current understanding of the physiological role of α-synuclein in the adult brain, and are important because
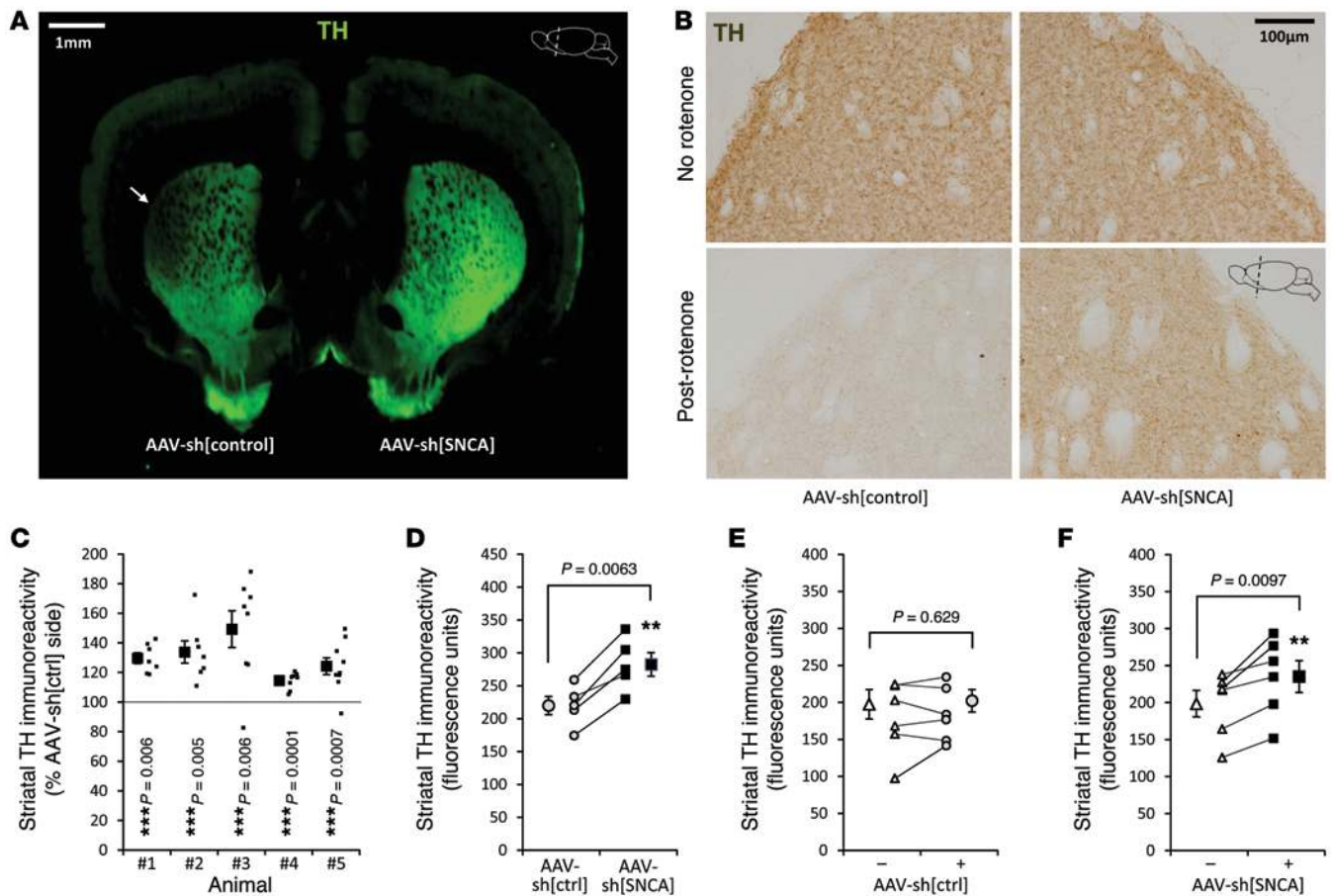
Figure 7. α-Synuclein knockdown protects striatal dopaminergic terminals in the rotenone model of Parkinson's disease. The integrity of striatal dopaminergic terminals was analyzed after rotenone exposure in cohort 4 (unilateral vector transduction, **E** and **F**) and cohort 5 (bilateral vector transduction, **A**–**D**). (**A**) Near-infrared immunofluorescence scan, showing TH expression (green) in a coronal section of the forebrain; the plane of the section is indicated in the inset. The white arrow shows loss of TH signal in the dorsolateral striatum on the AAV-sh[control] side; no lesion was seen on the AAV-sh[SNCA] side. Scale bar: 1 mm. (**B**) Forebrain sections were immunolabeled for TH expression (brown). The micrographs show the dorsolateral striatum on each side of brains from cohort 1 (upper panels; bilateral vector transduction, no rotenone) and cohort 5 (lower panels; bilateral vector transduction, post-rotenone). Scale bar (for all four panels): 100 μm. (**C**–**F**) Dorsolateral striatal TH signal was measured by quantitative near-infrared immunofluorescence. (**C**) Cohort 5: striatal TH signal on the AAV-sh[SNCA] side of each section is shown as a percentage of the signal measured on the AAV-sh[control] side of the same section. Small markers show individual sections; large markers show mean ± SEM for each animal. (**D**, **E**, and **F**) Mean striatal TH signal is shown for cohorts 5 (**D**) and 4 (**E** and **F**). The two sides from each animal are shown as small markers connected by lines; large markers show group mean ± SEM. **P < 0.01, ***P < 0.001, AAV-sh[SNCA] side versus contralateral side, 2-tailed paired *t* test.

they suggest that α-synuclein may be a valid therapeutic target for neuroprotection in PD.

In contrast to the MPTP models employed in previous studies, rotenone exposure causes a similar degree of mitochondrial inhibition in cells throughout the brain and outside the CNS (34). Despite this widespread mitochondrial impairment, neuropathology in rotenone-exposed animals is selective and resembles PD (34, 36, 39, 47). The model supports the idea that systemic abnormalities of mitochondrial complex I function, as reported in PD patients (15), can cause the specific pattern of neurodegeneration observed in PD. However, the mechanisms underlying the selective loss of specific neuronal populations in response to systemic mitochondrial dysfunction are unknown. Nigral dopaminergic neurons express *SNCA* mRNA more abundantly than adjacent cell groups (see Figure 2), and these high expression levels may be one factor in dictating degeneration of these neurons in PD. Our data showing that

α-synuclein knockdown has a neuroprotective effect in the rotenone model support the idea that α-synuclein expression levels can modulate the susceptibility of nigral dopaminergic neurons to chemicals that inhibit mitochondrial function. This is compatible with recent genome-wide association studies showing that *SNCA* gene variants (5–7) that may alter α-synuclein expression levels (8) were associated with enhanced risk of Parkinson's disease. Consequently, our findings may be relevant to understanding how genetic and environmental etiological factors converge to provoke PD pathogenesis. The mechanism linking α-synuclein with susceptibility to mitochondrial impairment in dopaminergic neurons is unclear. It is possible that endogenous α-synuclein compromises mitochondrial function, makes mitochondria more sensitive to inhibitors, mediates toxicity triggered by mitochondrial dysfunction, or alters cellular responses to abnormal mitochondrial function. It will be of considerable interest to address these possibilities experimentally.
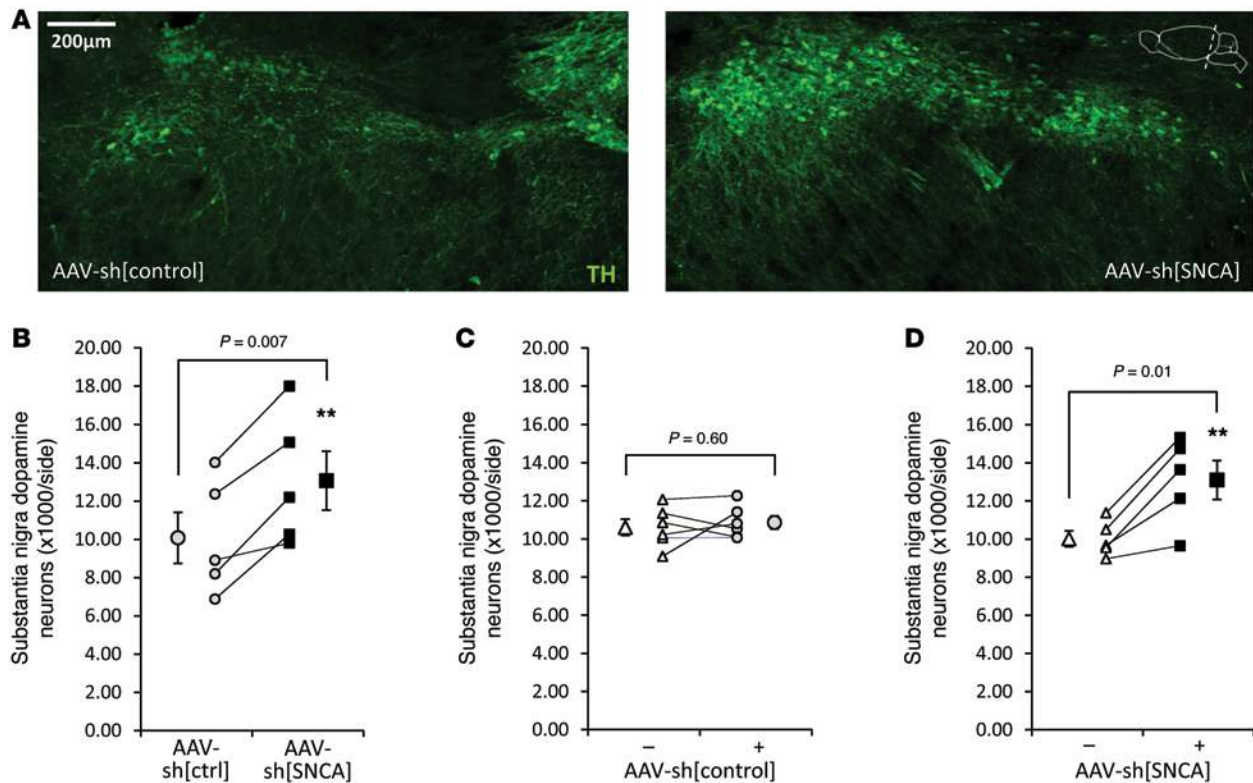
Figure 8. α-Synuclein knockdown protects substantia nigra dopaminergic neurons in the rotenone model of Parkinson's disease. The number of substantia nigra dopaminergic neurons remaining after chronic rotenone exposure was determine in cohorts 4 (unilateral vector transduction) and 5 (bilateral vector transduction). (**A**) Confocal micrographs show the substantia nigra from a representative midbrain section derived from a rat that received AAV-sh[control] on one side (left panel) and AAV-sh[SNCA] on the other (right panel) prior to chronic rotenone exposure. There was striking loss of dopaminergic neurons on the AAV-sh[control] side, as expected following chronic rotenone exposure using this regimen. In contrast, the AAV-sh[SNCA] side showed evidence of neuroprotection. Scale bar: 200 μm. (**B**–**D**) Unbiased stereology was used to determine the total number of remaining substantia nigra dopaminergic neurons on each side of the brain in cohorts 4 (unilateral vector transduction; **C** and **D**) and 5 (bilateral vector transduction; **B**). The stereological count for each individual animal is shown (small markers; data for the two sides of each brain are connected by a line). Large markers show the group mean ± SEM. White triangles, nontransduced side; gray circles, AAV-sh[control]–transduced side; black squares, AAV-sh[SNCA]–transduced side. **$P < 0.01$, 2-tailed paired t test, AAV-sh[SNCA] side versus contralateral side.

The discovery of pathogenic *SNCA* gene mutations in rare parkinsonism phenocopies (10, 12) and the prominence of α-synuclein pathology in sporadic PD (2, 48) led to consideration of shRNA targeting α-synuclein expression as a possible neuroprotective intervention in PD (49). However, this has been difficult to test in the absence of suitable models. Transgenic mice overexpressing α-synuclein have not been reported to develop robust degeneration of substantia nigra dopaminergic neurons, precluding their use to evaluate neuroprotective agents (including gene transfer vectors targeting *SNCA*) (50–55). The commonly employed MPTP and 6-OHDA toxin models of PD are associated with acute lesions that do not typically show synucleinopathy (56). Chronic exposure to MPTP did result in synucleinopathy (57), but attempts at therapeutic α-synuclein knockdown during adulthood have not been reported in this model. Furthermore, neither MPTP nor 6-OHDA has been etiologically associated with typical PD in humans. Occupational rotenone exposure is implicated as an environmental risk factor in typical sporadic PD (21), suggesting that the rotenone model of PD may have etiological (construct) validity. In addition, this model replicates numerous key features of PD, including progressive nigral dopaminergic neuron degeneration and α-synuclein pathology, suggesting that the model

also has face validity. By exploiting the rotenone model, we have demonstrated for the first time to our knowledge that knockdown of endogenous α-synuclein in the adult brain ameliorates PD-like neurodegeneration in vivo. This is an important finding with implications for translational research, because these data suggest that selective targeting of α-synuclein by shRNA may be a valid therapeutic approach for neuroprotection in sporadic PD.

Further consideration of shRNA gene delivery as a therapeutic approach will be influenced in part by the prospect of toxicity arising from loss of α-synuclein in the adult brain. Germline deletion of the *Snca* gene did not give rise to significant adverse effects; multiple independent murine *Snca*^{−/−} lines were viable and did not show overt nigral pathology (28, 29, 45, 58), although a recent study suggested that a developmental mechanism occurring between E10.5 and E13.5 caused the number of nigral dopaminergic neurons in *Snca*^{−/−} mice to be approximately 30% less than controls in one strain of *Snca*^{−/−} mice (59). Interestingly, some animal species, including zebrafish (60) and a naturally occurring murine strain (61), spontaneously lost the *Snca* gene without compromised survival or motor function. This suggests that α-synuclein may be dispensable, possibly due to compensa-
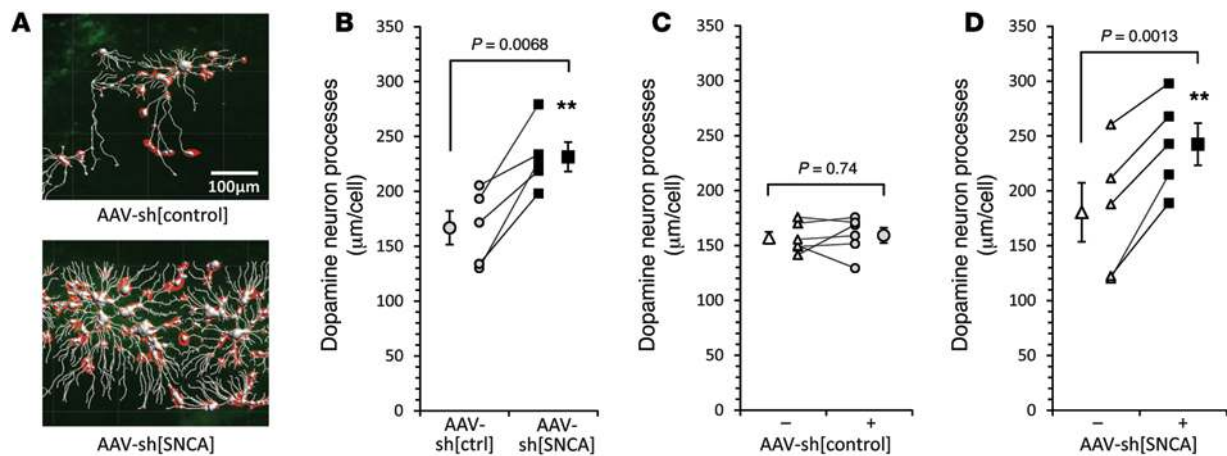
Figure 9. α-Synuclein knockdown protects substantia nigra dopaminergic neuron processes in the rotenone model of Parkinson's disease. The processes of substantia nigra dopaminergic neurons remaining after chronic rotenone exposure were evaluated in cohorts 4 (unilateral vector transduction; **C** and **D**) and 5 (bilateral vector transduction; **A** and **B**). (**A**) An automated tracing algorithm was used to identify TH-immunoreactive processes (white) and cell bodies (red). The pictures show two sides of the same section, from an animal that received AAV-sh[control] on one side (upper panel) and AAV-sh[SNCA] on the other (lower panel). The dendritic arbors of surviving dopaminergic neurons appeared compromised on the AAV-sh[control] side and relatively preserved on the AAV-sh[SNCA] side. Scale bar: 100 μm. (**B–D**) The total length of TH-immunoreactive processes per surviving TH+ neuron was measured on each side of the brain in animals from cohorts 5 (**B**) and 4 (**C** and **D**). Small markers show the mean for each individual animal (data for the two sides of each brain are connected by a line); large markers show group mean ± SEM. **$P < 0.01$, 2-tailed paired t test, AAV-sh[SNCA] side versus contralateral side.

tory functions of β- and γ-synucleins (62). However, acute knockdown of *Snca* in the adult brain could potentially cause unwanted effects by circumventing developmental compensatory mechanisms that occur in germline null mutants. There are four previous reports of RNAi-mediated knockdown of endogenous α-synuclein in the adult CNS in vivo (63–66). Naked siRNA infused into the mouse hippocampus gave rise to a significant 60%–80% reduction in *Snca* mRNA and a qualitative decrease in α-synuclein protein levels, but no overt cell loss or microgliosis (65). Naked siRNA infused into the primate midbrain caused a 50% reduction in *SNCA* mRNA, associated with a 40% reduction in α-synuclein. There was no inflammation, loss of nigral dopaminergic neurons, changes in the concentrations of striatal dopamine or its metabolites, or other toxicity (63). More recently, exosomes bearing a Lamp2b-RVG (rabies virus glycoprotein) fusion protein to target delivery to neurons were administered systemically in mice (66). Expression levels of α-synuclein were reduced in the midbrain (45%), striatum (43%), and cortex (24%) by 7 days after the procedure. No overt toxicity was noted, although motor function, neurochemistry, and histological end points for nigrostriatal integrity were not reported. Consistent with these previous reports, we observed no abnormalities in motor function, loss of striatal TH-expressing terminals, or loss of dopaminergic neurons or damage to their dendrites 6 weeks after AAV-sh[SNCA] transduction resulting in ≈35% knockdown of α-synuclein.

In contrast, a single previous study unexpectedly found rapidly progressive neurodegeneration in rats following AAV-mediated delivery of shRNA directed at the *Snca* transcript (64). TH-immunoreactive neurons were depleted in the nigra by more than 90% at 4 weeks after transduction, and this was associated with loss of striatal TH expression and asymmetric evoked motor function. It is unclear why these outcomes differ so dramatically from our work, and from other work employing naked siRNA

or exosome delivery to target the SNCA transcript. Although both AAV-shRNA studies (ref. 64 and the present work) used the same vector dose ($4 × 10^9$ vector genomes/side), there were multiple methodological differences: (i) The shRNA sequences differed between the studies. This may have influenced the level of knockdown or the possibility of off-target effects. (ii) The previous study used an AAV2/5 pseudotype to deliver shRNA, whereas we used AAV2. This may have changed the efficiency with which transgene DNA was delivered to neurons. (iii) The previous study used an H1 promoter to drive shRNA expression, whereas we employed a U6 promoter. This may have altered the relative expression levels of the shRNA in dopaminergic neurons. In combination, these methodological differences may account for the reported disparity in the level of α-synuclein knockdown: 70%–85% loss of nigral α-synuclein expression was found at 4 weeks after transduction in the previous study (64), compared with ≈35% knockdown at 6 weeks in the present work. Consequently, it is possible that the degree of acute α-synuclein knockdown determines whether toxicity occurs. An alternative interpretation is that the neurodegeneration reported previously may have been attributable to factors other than loss of α-synuclein. This is compatible with other work showing that an AAV-H1:shRNA vector targeting human, but not rat, *SNCA* was toxic in the rat substantia nigra (as was a similar vector expressing shRNA targeting luciferase), suggesting that nonspecific toxicity from shRNA expression at high levels may be important (67, 68). Regardless, the absence of neurodegeneration resulting from α-synuclein knockdown in our study is compatible with findings in a range of other model systems (28, 29, 45, 58, 61, 63). These data show that α-synuclein can be targeted in vivo in the adult brain without causing cell death.

Even though we did not observe dopaminergic cell loss in our study, the striatum ipsilateral to AAV-sh[SNCA] transduc-
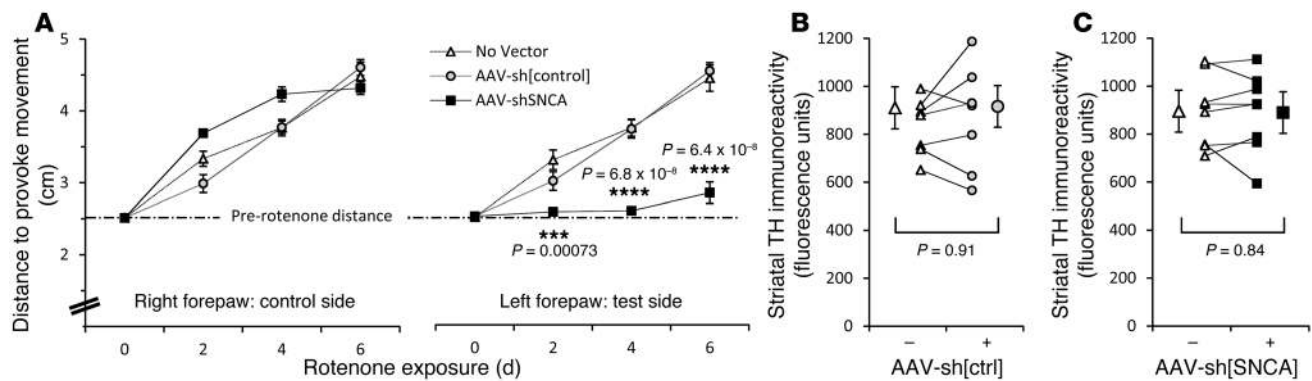
Figure 10. Rescue of dopaminergic function precedes degeneration of striatal terminals. Animals from cohort 6 received either AAV-sh[SNCA] (black squares) or AAV-sh[control] (gray circles) unilaterally in the substantia nigra or no vector (white triangles). Starting at 21 days after transduction, rats were administered rotenone 2.8 mg/kg/d via intraperitoneal injection for 6 days, after which brains were harvested for analysis. (**A**) A postural instability test was used to evaluate forelimb motor function during rotenone administration. Mean ± SEM distance to trigger a compensatory forelimb movement is shown for the right forepaw (controlled by nontransduced side of brain; left graph) and left forepaw (controlled by vector-transduced side of brain; right graph). ***$P < 0.001$, ****$P < 0.0000001$, left forepaw of AAV-sh[SNCA] group versus left forepaw of AAV-sh[control] or non-vector groups, one-way ANOVA. (**B** and **C**) Once motor asymmetry was clearly established in the AAV-sh[SNCA] group after 6 days of rotenone exposure, brains were analyzed for striatal dopaminergic terminal integrity. Quantitative near-infrared immunofluorescence was used to measure dorsolateral striatal TH expression on each side of 5–6 sections per animal. Small markers show the mean for each animal (+, vector side; –, nontransduced control side; lines join the means for the two sides of each brain); large markers show mean ± SEM for all eight animals in each group.

tion showed ≈20% decrease in dopamine level, which was not apparent following AAV-sh[control] transduction. This was not associated with detectable abnormalities of motor function, loss of TH immunoreactivity in the striatum, or enhanced dopamine turnover, suggesting that the striatal terminals of the transduced dopaminergic neurons were intact. Furthermore, we did not detect downregulation of TH (the rate-limiting enzyme for dopamine biosynthesis) in nigral neurons to account for the change in striatal dopamine level. Reduced dopamine levels in the absence of neurodegeneration have been reported in several different synuclein knockout and knockdown models (31, 45, 60). $Snca^{-/-}$ mice showed a 15%–20% reduction in striatal dopamine, but no significant change in the ratio of dopamine to its metabolites (45); this reduction was more prominent (36%) in aged animals (31). The mechanisms underlying these changes are unclear but are thought to reflect a reduction in dopamine synthesis, reuptake, or storage occurring in the absence of α-synuclein, as part of a wider picture of alterations in neurotransmitter handling at dopaminergic terminals. These data raise the intriguing possibility that functions of α-synuclein involved in dopamine handling and storage are relevant to the protection of dopaminergic terminal function that we observed as an early event in the rotenone model following α-synuclein knockdown. Dopamine oxidation products exert a highly deleterious effect on mitochondrial function (69), and it is conceivable that reduced dopamine stores in striatal terminals are one component of the neuroprotective effect of α-synuclein knockdown in the rotenone model.

In summary, this is the first demonstration to our knowledge that knockdown of endogenous α-synuclein in the adult substantia nigra attenuates motor deficits and neurodegeneration in an animal model of PD. Given the demonstrated safety of AAV2 vectors in human PD gene therapy trials, this approach has significant translational potential and should be evaluated further as a possible neuroprotective intervention.

Methods

Viral vectors. AAV-sh[SNCA] and AAV-sh[control] were generated by ligating annealed oligonucleotides encoding sh526 (Figure 1A) or a control sequence (5′-AATTCTCCGAACGTGTCACGT-3′) into the BamHI/EcoRI sites of pAAV-D(+)-U6-siRNA-CMV-GFP, which was derived from pAAV-D(+)-U6-siRNA-CMV-zsGreen (a gift from Bing Wang, University of Pittsburgh) by replacing the zsGreen open reading frame with GFP. Vectors were prepared to high titer and purity by plasmid co-transfection in 293 cells at the University of Pennsylvania Vector Core. Animals were anesthetized with isoflurane (induction 3%, maintenance 2%–3%). Viral vector delivery parameters were optimized for infusion site, delivery volume, rate of delivery, infusion needle type, vector type (lentivirus [ref. 40], herpes simplex virus, AAV [AAV2, -2/1, -2/9]) (Supplemental Figure 4), vector concentration, and number of infusions in a series of pilot experiments. In the experiments shown, 2 μl viral vector suspension was infused dorsal to the substantia nigra (–5.8 mm anterior/posterior, ±2.2 mm right/left, –7.5 mm ventral to bregma) using a Hamilton syringe with a 30-gauge needle (45° bevel) at a rate of 0.2 μl/min. AAV-sh[SNCA] and AAV-[control] were used at the same concentration, 2.0×10^{12} GC/ml, total dose 4.0×10^{9} GC/side.

Animals. Adult male Lewis rats of approximately 6 months of age were obtained from Hilltop Lab Animals and Charles River.

Rotenone. Animals in cohorts 1, 2, and 3 were evaluated without rotenone treatment 21 or 42 days after viral vector infusion. Animals in cohorts 4, 5, and 6 received daily intraperitoneal rotenone (2.8 mg/kg/d) (36) starting 21 days after vector infusion. Animals were monitored daily for weight loss and motor signs, and rotenone was continued until the experimental end point defined by weight loss of >20% or severe bilateral bradykinesia. Motor tests were carried out every 2 days during rotenone exposure and were performed exactly as published in our previous work (36).

Neurochemistry. Striatal tissue samples were sonicated on ice in 0.1 M perchloric acid and centrifuged for 30 minutes at 16,100 *g*. The supernatant was collected and filtered in Costar Spin-X 0.22-μM nylon

membrane polypropylene centrifuge tubes at 1,000 *g*, then injected into a Waters 2695 HPLC separation module at 4°C. The HPLC mobile phase consisted of 0.05 M sodium phosphate, 0.01 M citric acid, 0.01 M sodium acetate, 10% methanol, 0.32 mM octyl sulfate sodium salt, 0.1 mM ethylendiaminetetraacetic acid, pH 2.5. The flow rate was 0.8 ml/min. Neurotransmitters were separated on a Varian Microsorb-MVC18 4.6 × 250–mm column with a 5-μm particle size and detected on a Waters 2465 electrochemical detector with a glassy carbon electrode set at 750 mV referenced to an ISAAC electrode at 28°C. Quantification was carried out by comparison with high purity standards.

Histology. Animals were deeply anesthetized with pentobarbital (50 mg/kg) and perfused-fixed with PBS and 4% paraformaldehyde. Brains were post-fixed, cryoprotected, and sectioned (35 μm) using a sliding freezing-stage microtome. Dopaminergic terminal density in the striatum was determined by measuring TH immunofluorescence as previously described (40) (Supplemental Figure 6). Antibodies were primary mouse anti-TH (1:2,000; 48 hours at 4°C; Millipore, MAB318); and secondary donkey anti-mouse (1:500; 2 hours at 20°C; LI-COR, IRDye 800CW). Sections were imaged using a LI-COR infrared scanner. Regions of interest were drawn in the striatum as shown in Supplemental Figure 6, and mean fluorescence intensity was calculated. To quantify α-synuclein expression in nigral neurons, midbrain sections were colabeled for GFP to identify transduced neurons (1:4,000; Millipore, MAB3580; secondary Alexa Fluor 488–anti-mouse, 1:500); tyrosine hydroxylase to identify dopaminergic neurons (1:2,000; Millipore, AB152; secondary Cy3–anti-rabbit, 1:500); and α-synuclein (1:3,000; Millipore, AB5334P; secondary Cy5–anti-sheep, 1:500). Images were acquired using an Olympus FV-1000 confocal microscope, with constant laser and detector settings that were optimized to avoid saturation in the α-synuclein and TH channels. Regions of interest were drawn around at least 60 transduced (GFP+) dopaminergic (TH+) neurons on each side of each animal, allowing calculation of mean α-synuclein and TH immunofluorescence.

Unbiased stereology. One in every six coronal midbrain sections was immunolabeled for MAP2 (1:2,000, Millipore; secondary Alexa Fluor 647–anti-mouse, 1:500, Invitrogen) and TH (1:3,000, Millipore, secondary Cy3–anti-sheep, 1:500, Jackson ImmunoResearch Laboratories Inc.). Images were acquired using an automated Nikon 90i upright widefield microscope with a 20× objective (NA 0.75), equipped with a linear-encoded motorized stage and Qimaging Retiga cooled CCD camera. Micrographs were analyzed using NIS-Elements software. A region of interest was drawn around the substantia nigra, and neurons were quantified by a single investigator blinded to whether the animals had received rotenone or viral vector. The software counted all cells in which MAP2-, TH-, and H33342-positive nuclei coincided. The method yields identical results to manual stereology, but has a lower coefficient of error (<0.05 for each animal) owing to the much greater number of neurons sampled (70, 71). Neurite architecture was analyzed using the automated Surpass FilamentTracer module of Imaris software (version 7.1.1, Bitplane), employing a skeletonized algorithm.

RNA in situ hybridization. AAV-sh[SNCA]–induced nigral *Snca* knockdown was verified by RNA in situ hybridization in midbrain sections from all animals of cohorts 1, 2, 4, 5, and 6. Probe templates were amplified from rat brain RNA by RT-PCR using primers to *Snca* (F: 5′-AGATGGATGTGTTCATGAAAG-3′, R: 5′-TCGT-TAGGCTTCAGGCTCATA-3′); *Sncb* (F: 5′-CCGCCAGGATGGACGT-GTTCAT-3′, R: 5′-ATGGACCCTTACGCCTCTGGCT-3′); and *Sncg* (F:

5′-AGCAGCCAGGTCTCTTCCTC-3′, R: 5′-TGGAAGCCTTCTAGT-CACCT-3′). Products were cloned and sequence verified. Digoxigenin-labeled cRNA probes were generated by in vitro transcription of linearized plasmid. Fixed, free-floating brain sections were washed in PBS, then treated with 0.1% diethylpyrocarbonate (DEPC) in PBS for 15 minutes ×2, equilibrated in 5× SSC, postfixed in 4% PFA, and washed in PBS. Sections were then incubated in ULTRAhyb (Ambion) supplemented with 1 mg/ml Torula RNA (Sigma-Aldrich) for 1 hour at 68°C. Labeled cRNA probe was then added to a final concentration of 150 ng/ml and hybridized at 68°C overnight. Hybridization buffer and unbound probe were removed by washing in 2× SSC; stringency washes were carried out at 68°C in 0.1× SSC. Hybridized probe was localized using alkaline phosphatase–conjugated (AP-conjugated) anti-digoxigenin antibody (Roche) and bound antibody detected by a histochemical reaction using an AP substrate (BM Purple, Roche).

Statistics. Experiments were powered to detect >10% differences in histological and neurochemical end points between treatment conditions and >20% differences in behavioral end points, with α = 0.05 and β = 0.8, using expected effect sizes and variances estimated from our pilot studies. Two-tailed paired *t* test was employed to compare morphological end points, protein expression data, and neurochemical measurements from the two sides of the same brains. One-way ANOVA with Tukey's post hoc test was used to compare motor function and weight of different animals from multiple treatment groups. One-way ANOVA (three experimental groups) or two-tailed unpaired *t* test assuming unequal variance (two experimental groups) was used to compare histological end points from separate animals in different experimental groups. Categorical data were analyzed using a χ^2 test. Survival data were analyzed using a log-rank test.

Study approval. Experiments were approved by the Institutional Animal Care and Use Committees of both the Pittsburgh Veterans' Affairs Healthcare System and the University of Pittsburgh.

Acknowledgments

Address correspondence to: Edward A. Burton, University of Pittsburgh, 7015 BST-3, 3501 Fifth Avenue, Pittsburgh, Pennsylvania 15213, USA. Phone: 412.648.8480; E-mail: eab25@pitt.edu.

Jason R. Cannon's present address is: School of Health Sciences, Purdue University, West Lafayette, Indiana, USA.

Amina El Ayadi's present address is: Department of Surgery, University of Texas Medical Branch, Galveston, Texas, USA.

Alevtina D. Zharikov, Jason R. Cannon, and Victor Tapias contributed equally to this work and are co–first authors.

1. Braak H, Braak E. Pathoanatomy of Parkinson's disease. *J Neurol*. 2000;247 Suppl 2:II3–10.
2. Spillantini MG, Schmidt ML, Lee VM, Trojanowski JQ, Jakes R, Goedert M. Alpha-synuclein in Lewy bodies. *Nature*. 1997;388(6645):839–840.
3. Baba M, et al. Aggregation of alpha-synuclein in Lewy bodies of sporadic Parkinson's disease and dementia with Lewy bodies. *Am J Pathol*. 1998;152(4):879–884.
4. Spillantini MG, Crowther RA, Jakes R, Hasegawa M, Goedert M. alpha-Synuclein in filamentous inclusions of Lewy bodies from Parkinson's disease and dementia with lewy bodies. *Proc Natl Acad Sci U S A*. 1998;95(11):6469–6473.
5. Simon-Sanchez J, et al. Genome-wide association study reveals genetic risk underlying Parkinson's disease. *Nat Genet*. 2009;41(12):1308–1312.
6. Edwards TL, et al. Genome-wide association study confirms SNPs in SNCA and the MAPT region as common risk factors for Parkinson disease. *Ann Hum Genet*. 2010;74(2):97–109.
7. Satake W, et al. Genome-wide association study identifies common variants at four loci as genetic risk factors for Parkinson's disease. *Nat Genet*. 2009;41(12):1303–1307.
8. Fuchs J, et al. Genetic variability in the SNCA gene influences alpha-synuclein levels in the blood and brain. *FASEB J*. 2008;22(5):1327–1334.
9. Chartier-Harlin MC, et al. Alpha-synuclein locus duplication as a cause of familial Parkinson's disease. *Lancet*. 2004;364(9440):1167–1169.
10. Singleton AB, et al. alpha-Synuclein locus triplication causes Parkinson's disease. *Science*. 2003;302(5646):841.
11. Miller DW, et al. Alpha-synuclein in blood and brain from familial Parkinson disease with SNCA locus triplication. *Neurology*. 2004;62(10):1835–1838.
12. Polymeropoulos MH, et al. Mutation in the alpha-synuclein gene identified in families with Parkinson's disease. *Science*. 1997;276(5321):2045–2047.
13. Kruger R, et al. Ala30Pro mutation in the gene encoding alpha-synuclein in Parkinson's disease. *Nat Genet*. 1998;18(2):106–108.
14. Zarranz JJ, et al. The new mutation, E46K, of alpha-synuclein causes Parkinson and Lewy body dementia. *Ann Neurol*. 2004;55(2):164–173.
15. Schapira AH, Cooper JM, Dexter D, Jenner P, Clark JB, Marsden CD. Mitochondrial complex I deficiency in Parkinson's disease. *Lancet*. 1989;1(8649):1269.
16. Krige D, Carroll MT, Cooper JM, Marsden CD, Schapira AH. Platelet mitochondrial function in Parkinson's disease. The Royal Kings and Queens Parkinson Disease Research Group. *Ann Neurol*. 1992;32(6):782–788.
17. Jenner P. Oxidative stress in Parkinson's disease. *Ann Neurol*. 2003;53(Suppl 3):S26–S36.
18. Kitada T, et al. Mutations in the parkin gene cause autosomal recessive juvenile parkinsonism. *Nature*. 1998;392(6676):605–608.
19. Valente EM, et al. Hereditary early-onset Parkinson's disease caused by mutations in PINK1. *Science*. 2004;304(5674):1158–1160.
20. Bonifati V, et al. Mutations in the DJ-1 gene associated with autosomal recessive early- onset par-

kinsonism. *Science*. 2003;299(5604):256–259.
21. Tanner CM, et al. Rotenone, paraquat, and Parkinson's disease. *Environ Health Perspect*. 2011;119(6):866–872.
22. Heikkila RE, Manzino L, Cabbat FS, Duvoisin RC. Protection against the dopaminergic neurotoxicity of 1-methyl-4-phenyl-1,2,5,6-tetrahydropyridine by monoamine oxidase inhibitors. *Nature*. 1984;311(5985):467–469.
23. Devi L, Raghavendran V, Prabhu BM, Avadhani NG, Anandatheerthavarada HK. Mitochondrial import and accumulation of alpha-synuclein impair complex I in human dopaminergic neuronal cultures and Parkinson disease brain. *J Biol Chem*. 2008;283(14):9089–9100.
24. Hsu LJ, et al. alpha-synuclein promotes mitochondrial deficit and oxidative stress. *Am J Pathol*. 2000;157(2):401–410.
25. Sherer TB, et al. An in vitro model of Parkinson's disease: linking mitochondrial impairment to altered alpha-synuclein metabolism and oxidative damage. *J Neurosci*. 2002;22(16):7006–7015.
26. Paxinou E, et al. Induction of alpha-synuclein aggregation by intracellular nitrative insult. *J Neurosci*. 2001;21(20):8053–8061.
27. Klivenyi P, et al. Mice lacking alpha-synuclein are resistant to mitochondrial toxins. *Neurobiol Dis*. 2006;21(3):541–548.
28. Schluter OM, et al. Role of alpha-synuclein in 1-methyl-4-phenyl-1,2,3,6-tetrahydropyridine-induced parkinsonism in mice. *Neuroscience*. 2003;118(4):985–1002.
29. Dauer W, et al. Resistance of alpha-synuclein null mice to the parkinsonian neurotoxin MPTP. *Proc Natl Acad Sci U S A*. 2002;99(22):14524–14529.
30. Javitch JA, D'Amato RJ, Strittmatter SM, Snyder SH. Parkinsonism-inducing neurotoxin, N-methyl-4-phenyl-1,2,3,6 -tetrahydropyridine: uptake of the metabolite N-methyl-4-phenylpyridine by dopamine neurons explains selective toxicity. *Proc Natl Acad Sci U S A*. 1985;82(7):2173–2177.
31. Al-Wandi A, Ninkina N, Millership S, Williamson SJ, Jones PA, Buchman VL. Absence of alpha-synuclein affects dopamine metabolism and synaptic markers in the striatum of aging mice. *Neurobiol Aging*. 2010;31(5):796–804.
32. Chadchankar H, Ihalainen J, Tanila H, Yavich L. Decreased reuptake of dopamine in the dorsal striatum in the absence of alpha-synuclein. *Brain Res*. 2011;1382:37–44.
33. Fountaine TM, Wade-Martins R. RNA interference-mediated knockdown of alpha-synuclein protects human dopaminergic neuroblastoma cells from MPP(+) toxicity and reduces dopamine transport. *J Neurosci Res*. 2007;85(2):351–363.
34. Betarbet R, Sherer TB, MacKenzie G, Garcia-Osuna M, Panov AV, Greenamyre JT. Chronic systemic pesticide exposure reproduces features of Parkinson's disease. *Nat Neurosci*. 2000;3(12):1301–1306.
35. Sherer TB, Betarbet R, Kim JH, Greenamyre JT. Selective microglial activation in the rat rotenone model of Parkinson's disease. *Neurosci Lett*. 2003;341(2):87–90.
36. Cannon JR, Tapias V, Na HM, Honick AS, Drolet RE, Greenamyre JT. A highly reproducible rotenone model of Parkinson's disease. *Neurobiol Dis*. 2009;34(2):279–290.

37. Drolet RE, Cannon JR, Montero L, Greenamyre JT. Chronic rotenone exposure reproduces Parkinson's disease gastrointestinal neuropathology. *Neurobiol Dis*. 2009;36(1):96–102.
38. Cicchetti F, Drouin-Ouellet J, Gross RE. Environmental toxins and Parkinson's disease: what have we learned from pesticide-induced animal models? *Trends Pharmacol Sci*. 2009;30(9):475–483.
39. Johnson ME, Bobrovskaya L. An update on the rotenone models of Parkinson's disease: Their ability to reproduce the features of clinical disease and model gene-environment interactions. *Neurotoxicology*. 2015;46C:101–116.
40. Cannon JR, Sew T, Montero L, Burton EA, Greenamyre JT. Pseudotype-dependent lentiviral transduction of astrocytes or neurons in the rat substantia nigra. *Exp Neurol*. 2011;228(1):41–52.
41. LeWitt PA, et al. AAV2-GAD gene therapy for advanced Parkinson's disease: a double-blind, sham-surgery controlled, randomised trial. *Lancet Neurol*. 2011;10(4):309–319.
42. Marks WJ Jr, et al. Gene delivery of AAV2-neurturin for Parkinson's disease: a double-blind, randomised, controlled trial. *Lancet Neurol*. 2010;9(12):1164–1172.
43. Schallert T, Tillerson JL. Intervention strategies for degeneration of dopamine neurons in parkinsonism: optimizing behavioral assessment of outcome. In: Emerich DF, Dean RL, Sanberg PR, eds. *Central Nervous System Diseases: Innovative Animal Models from Lab to Clinic*. Totowa, New Jersey, USA: Humana Press; 2000:131–151.
44. Woodlee MT, Kane JR, Chang J, Cormack LK, Schallert T. Enhanced function in the good forelimb of hemi-parkinson rats: compensatory adaptation for contralateral postural instability? *Exp Neurol*. 2008;211(2):511–517.
45. Abeliovich A, et al. Mice lacking alpha-synuclein display functional deficits in the nigrostriatal dopamine system. *Neuron*. 2000;25(1):239–252.
46. Marella M, Seo BB, Nakamaru-Ogiso E, Greenamyre JT, Matsuno-Yagi A, Yagi T. Protection by the NDI1 gene against neurodegeneration in a rotenone rat model of Parkinson's disease. *PLoS ONE*. 2008;3(1):e1433.
47. Sherer TB, Kim JH, Betarbet R, Greenamyre JT. Subcutaneous rotenone exposure causes highly selective dopaminergic degeneration and alpha-synuclein aggregation. *Exp Neurol*. 2003;179(1):9–16.
48. Braak H, Del Tredici K, Bratzke H, Hamm-Clement J, Sandmann-Keil D, Rub U. Staging of the intracerebral inclusion body pathology associated with idiopathic Parkinson's disease (preclinical and clinical stages). *J Neurol*. 2002;249(Suppl 3):III/1–5.
49. Burton EA, Glorioso JC, Fink DJ. Gene therapy progress and prospects: Parkinson's disease. *Gene Ther*. 2003;10(20):1721–1727.
50. Kahle PJ, et al. Selective insolubility of alpha-synuclein in human Lewy body diseases is recapitulated in a transgenic mouse model. *Am J Pathol*. 2001;159(6):2215–2225.
51. Matsuoka Y, et al. Lack of nigral pathology in transgenic mice expressing human alpha-synuclein driven by the tyrosine hydroxylase promoter. *Neurobiol Dis*. 2001;8(3):535–539.
52. Lee MK, et al. Human alpha-synuclein-harboring familial Parkinson's disease-linked Ala-53 --> Thr

mutation causes neurodegenerative disease with alpha-synuclein aggregation in transgenic mice. *Proc Natl Acad Sci U S A*. 2002;99(13):8968–8973.

53. Neumann M, et al. Misfolded proteinase K-resistant hyperphosphorylated alpha-synuclein in aged transgenic mice with locomotor deterioration and in human alpha-synucleinopathies. *J Clin Invest*. 2002;110(10):1429–1439.

54. Gispert S, et al. Transgenic mice expressing mutant A53T human alpha-synuclein show neuronal dysfunction in the absence of aggregate formation. *Mol Cell Neurosci*. 2003;24(2):419–429.

55. Gomez-Isla T, et al. Motor dysfunction and gliosis with preserved dopaminergic markers in human alpha-synuclein A30P transgenic mice. *Neurobiol Aging*. 2003;24(2):245–258.

56. Halliday G, et al. No Lewy pathology in monkeys with over 10 years of severe MPTP Parkinsonism. *Mov Disord*. 2009;24(10):1519–1523.

57. Fornai F, et al. Parkinson-like syndrome induced by continuous MPTP infusion: convergent roles of the ubiquitin-proteasome system and alpha-synuclein. *Proc Natl Acad Sci U S A*. 2005;102(9):3413–3418.

58. Cabin DE, et al. Synaptic vesicle depletion correlates with attenuated synaptic responses to prolonged repetitive stimulation in

mice lacking alpha-synuclein. *J Neurosci*. 2002;22(20):8797–8807.

59. Garcia-Reitboeck P, et al. Endogenous alpha-synuclein influences the number of dopaminergic neurons in mouse substantia nigra. *Exp Neurol*. 2013;248:541–545.

60. Milanese C, et al. Hypokinesia and reduced dopamine levels in zebrafish lacking beta- and gamma1-synucleins. *J Biol Chem*. 2012;287(5):2971–2983.

61. Specht CG, Schoepfer R. Deletion of the alpha-synuclein locus in a subpopulation of C57BL/6J inbred mice. *BMC Neurosci*. 2001;2:11.

62. Burre J, Sharma M, Tsetsenis T, Buchman V, Etherton MR, Sudhof TC. Alpha-synuclein promotes SNARE-complex assembly in vivo and in vitro. *Science*. 2010;329(5999):1663–1667.

63. McCormack AL, Mak SK, Henderson JM, Bumcrot D, Farrer MJ, Di Monte DA. Alpha-synuclein suppression by targeted small interfering RNA in the primate substantia nigra. *PLoS ONE*. 2010;5(8):e12122.

64. Gorbatyuk OS, et al. In vivo RNAi-mediated alpha-synuclein silencing induces nigrostriatal degeneration. *Mol Ther*. 2010;18(8):1450–1457.

65. Lewis J, et al. In vivo silencing of alpha-synuclein using naked siRNA. *Mol Neurodegener*. 2008;3:19.

66. Cooper JM, et al. Systemic exosomal siRNA delivery reduced alpha-synuclein aggregates in brains of transgenic mice. *Mov Disord*. 2014;29(12):1476–1485.

67. Khodr CE, et al. An alpha-synuclein AAV gene silencing vector ameliorates a behavioral deficit in a rat model of Parkinson's disease, but displays toxicity in dopamine neurons. *Brain Res*. 2011;1395:94–107.

68. Han Y, Khodr CE, Sapru MK, Pedapati J, Bohn MC. A microRNA embedded AAV alpha-synuclein gene silencing vector for dopaminergic neurons. *Brain Res*. 2011;1386:15–24.

69. Berman SB, Hastings TG. Dopamine oxidation alters mitochondrial respiration and induces permeability transition in brain mitochondria: implications for Parkinson's disease. *J Neurochem*. 1999;73(3):1127–1137.

70. Tapias V, Greenamyre JT, Watkins SC. Automated imaging system for fast quantitation of neurons, cell morphology and neurite morphometry in vivo and in vitro. *Neurobiol Dis*. 2013;54:158–168.

71. Tapias V, Greenamyre JT. A rapid and sensitive automated image-based approach for in vitro and in vivo characterization of cell morphology and quantification of cell number and neurite architecture. *Curr Protoc Cytom*. 2014;68:12.33.1–12.33.22.